Production of Nitric Oxide within the *Aplysia californica* Nervous System

Xiaoying Ye, Fang Xie, Elena V. Romanova, Stanislav S. Rubakhin, and Jonathan V. Sweedler*

Department of Chemistry and the Beckman Institute. University of Illinois, Urbana, Illinois 61801

Abstract

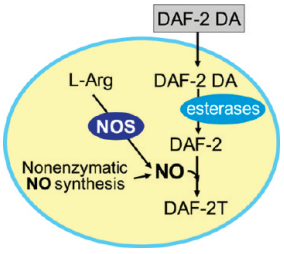

Nitric oxide (NO), an intercellular signaling molecule, helps coordinate neuronal network activity. Here we examine NO generation in the *Aplysia californica* central nervous system using 4,5-diaminofluorescein diacetate (DAF-2 DA), a fluorescent reagent that forms 4,5-diaminofluorescein triazole (DAF-2T) upon reaction with NO. Recognizing that other fluorescence products are formed within the biochemically complex intracellular environment, we validate the observed fluorescence as being from DAF-2T; using both capillary electrophoresis and mass spectrometry we confirm that DAF-2T is formed from tissues and cells exposed to DAF-2 DA. We observe three distinct subcellular distributions of fluorescence in neurons exposed to DAF-2 DA. The first shows uniform fluorescence inside the cell, with these cells being among previously confirmed NO synthase (NOS)-positive regions in the *Aplysia* cerebral ganglion. The second, seen inside buccal neurons, exhibits point sources of fluorescence, 1.5 ± 0.7 μm in diameter. Interestingly, the number of fluorescence puncta increases when the tissue is preincubated with the NOS substrate L-arginine, and they disappear when cells are preexposed to the NOS inhibitor L-nitro-arginine methyl ester (L-NAME), demonstrating that the fluorescence is connected to NOS-dependent NO production. The third distribution type, seen in the R2 neuron, also exhibits fluorescent puncta but only on the cell surface. Fluorescence is also observed in the terminals of cultured bag cell neurons loaded with DAF-2 DA. Surprisingly, fluorescence at the R2 surface and bag cell neuron terminals is not modulated by L-arginine or L-NAME, suggesting that it has a source distinct from the buccal and cerebral ganglion DAF 2T-positive tissues.

Keywords: Nitric oxide, nitric oxide synthase, fluorescence imaging, DAF-2 DA, *Aplysia* CNS, capillary electrophoresis

Nitric oxide (NO) is an important intercellular signaling molecule with a wide range of neuronal functions in the central nervous system (CNS) (*1*−*6*). NO is produced by a family of enzymes, the NO synthases (NOSs). However, NOS-positive neurons are reported to represent only 1% of neuronal cells in the brain (*7*−*9*). Therefore, identifying nitrergic neurons and characterizing their cellular physiology and biochemistry at subcellular levels are integral to furthering our understanding of this highly reactive molecule. *Aplysia* and related opisthobranch mollusks are well-suited to studying NO signaling; their neurons are typically large, individually identifiable, and easily accessible. As a result, many of the underlying principles governing the mechanisms of neuronal activity have been elucidated through studies of this invertebrate system (*10*).

NO has been proposed as an important regulator involved in molluscan feeding behavior and neuronal plasticity (*11*−*13*). The distribution of putative NOS-containing cells in the *Aplysia* CNS has been characterized by NADPH-diaphorase (NADPH-d) staining (*14*−*17*). Although NADPH-d can indicate the presence of a diaphorase-dependent enzyme activity, it can be difficult to determine staining specificity. Thus, one normally does not consider NADPH-d staining as being from NO if it fails to follow known NOS pharmacology. Therefore, if unusual NO sources are observed, they would be presumed to be artifacts. Because limited NOS molecular information is available in *Aplysia*, genetic tools are not available, although this situation will change as the *Aplysia californica* genome project is finalized.

Among analytical techniques for measuring NOS activity, fluorescence and electrochemical methods have

Received Date: September 11, 2009
Revised Manuscript Received: November 16, 2009
Published on Web Date: December 03, 2009

DOI: 10.1021/cn900016z | *ACS Chem. Neurosci.* (2010), *1*, 182–193

the required sensitivity to achieve NO detection at the single-cell level (*18*, *19*). Electrochemical sensors, such as miniature-sized microelectrodes, work well when placed near the NO source, such as the cell surface, to monitor localized surface concentrations and to follow the dynamics of NO production (*20*, *21*). Electrodes of various materials have been fabricated to increase response speed and sensitivity (*20*) and novel permselective coating membranes have been developed to increase the electrode selectivity (*22*). On the other hand, fluorescence approaches are well-suited for intracellular imaging of NO production in living cells. Both approaches can be coupled with separation techniques such as capillary electrophoresis (CE) and liquid chromatography (LC) to improve detection sensitivity and specificity. Since NO does not itself fluoresce, several fluorescent dyes have been designed and applied to NO measurements for biological systems, including organic (*23*, *24*) and genetically encoded fluorescent indicators (*25*). Previously, we employed 4,5-diaminofluorescein (DAF-2) to determine NO production in mammalian cells (*26*). This NO-specific indicator was developed in 1998 (*24*) and is now extensively used. However, until now, the direct measurement of NO in molluscan neurons using DAF-2 had been confined to analyses of the contents of isolated putative NOS-containing neurons by reacting their contents with DAF-2 offline, separating the cellular analytes, and detecting the NO-related signals (*27*, *28*).

Here we examine several distinct NO-producing neurons in the *A. californica* CNS, determine the subcellular localization of NO generation, and test its pharmacology. We characterize NO production in physiologically active invertebrate neurons using the cell membrane-permeable form of DAF-2, 4,5-diaminofluorescein diacetate (DAF-2 DA). Semi-intact preparations of *A. californica* CNS regions, as well as cultured neurons, were loaded with this fluorescent indicator in an environment that preserves their activity. The DAF-2 DA-loaded neurons demonstrated different patterns of fluorescence; in some, the fluorescence was altered by pharmacological modulators of known NO-producing biochemical pathways and in others, it was independent of pharmacological modulation.

Because our results provide evidence for several distinct NO sources having different cellular distributions and unique pharmacological profiles, we carefully validated our choice of fluorescent probe. We isolated the neurons and performed single-cell microanalytical measurements of DAF-related compounds. Both diaminofluorescein and the diaminorhodamine probes are known to produce multiple fluorescence products (*29*). Therefore, using CE and mass spectrometry (MS), we confirmed that a portion of the fluorescence resulted from the reaction of DAF-2 with NO. It appears, based on their subcellular distributions and pharmacologies, that there are distinct sources of NO in the *A. californica* CNS.

Results and Discussion

Detection of DAF-2 and DAF-2 DA from *A. californica* Cells

Investigation of NO distribution in the nervous system often relies on mapping NOS localization but not in direct NO detection. Although useful, NOS observation presents an incomplete picture of NO production because the presence of the enzyme does not necessarily correlate to imply NO production and NOS alone does not account for possible nonenzymatic NO production. Therefore, direct and specific sensors for NO such as DAF-2 (*24*) may alleviate these challenges.

In this work, we used the membrane-permeable form of DAF-2, DAF-2 DA, to investigate intracellular NO generation within cells from the widely studied neurobiological model *Aplysia californica*. Intracellular loading of DAF-2 is an effective approach for imaging subcellular NO distribution in the CNS. Unfortunately, DAF-2 cannot pass the plasma membrane without treating the cells, with either intracellular injection, electroporation, or a detergent. In contrast, DAF-2 DA is a cell-membrane-permeable form of DAF-2. It contains two acetate groups attached to the COO^- groups through ester bonds and readily passes across the lipid bilayer. Typically, once inside the cells, the acetate group is cleaved off of DAF-2 DA by esterases located in the cytosol. DAF-2 DA is thus converted to DAF-2, which reacts with endogenously or exogenously generated NO to form the fluorescent product DAF-2T (Figure 1). Despite the substantial contributions of DAF-2 DA to imaging NO production in mammalian cells, this molecular sensor has yet to be applied to molluscan neurons.

The mechanism of DAF-2/DAF-2 DA conversion shares similarities with that of the calcium fluorescent sensors, fura-2 and fura-2 acetoxymethyl ester (*30*, *31*). The latter recently has been applied to various molluscan models such as *Aplysia punctata* (*32*), *Lymnaea stagnalis* (*33*), and *Bulla gouldiana* (*34*). Using a similar approach, we injected metacerebral and F-cluster neurons from the cerebral ganglia of *A. californica* with DAF-2 solution, supplemented with a green triarylmethane dye, fast green FCF, which gives neurons a distinct green color and serves as an indicator of successful injection. The physiological status of neurons during and after injection was monitored by electrophysiological recording. The tested DAF-2 concentration in the injected solution ranged from 10 μM to 2 mM. However, no significant fluorescence was observed in

DOI: 10.1021/cn900016z | *ACS Chem. Neurosci.* (2010), *1*, 182–193

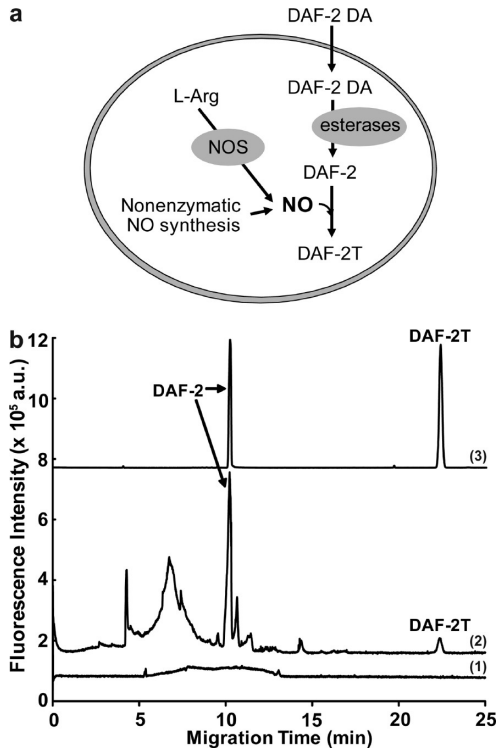

Figure 1. (A) Schematic illustration of the mechanisms involved in intracellular fluorescence NO detection using DAF-2 DA. (B) CE-LIF profiles of the conversion of DAF-2 DA to DAF-2 in the *Aplysia* CNS: (a) electropherogram of DAF-2 DA in ASW solution incubated for 1 h. DAF-2 DA alone does not produce detectable fluorescence; (b) electropherogram shows that DAF-2 DA is converted to DAF-2 after incubating DAF-2 DA with cell lysate for 10 min; (c) representative electropherogram of 10 μM DAF-2 reacting with 1 μM NO in pH = 7.4 ± 0.1 sodium phosphate buffer (reaction time is 20 min).

the DAF-2-loaded neurons compared with those injected with fast green only ($N = 3$).

In contrast to the DAF-2 microinjection studies, which did not produce evidence regarding NO production, the experiments involving ganglia incubation in the DAF-2 DA solutions showed prominent DAF-2T signals. NO-producing neurons are located in different CNS regions and exhibit various morphologies. The C2 neuron, located in the E-cluster of the cerebral ganglion, has previously been confirmed as NOS-positive by both NADPH-d staining and NOS *in situ* hybridization. The neuropil in this area shows much more intense fluorescence, indicating that much of the NO production may be extrasomatic. Here, using the DAF-2 DA detection approach, we also observed fluorescence in neurons and neuropil located in the E-cluster ($N = 3$ trials), although we have not identified specific neurons within the cluster. Most of the large neurons in *Aplysia* ganglia do not fluoresce natively at the wavelength employed for DAF-2T detection, indicating that the fluorescence is due to DAF-related products. In some cases, the fluorescence was not consistent; as an example, for the metacerebral (MCC) neuron, faint fluorescence was only observed in one of ten preparations. Although some small and medium-sized neurons showed intense uniform fluorescence, it was not consistently observed.

It has also been reported that in the *Aplysia* CNS, most NADPH-d reactivity is associated with the neuropil, with the highest density of glomeruli-like NADPH-d-reactive zones in the areas of neurite termini (*16*). We have also found scattered fluorescence in areas of connective tissue that may contain some termini (Figure S1, Supporting Information, $N = 5$), findings that concur with previously reported data (*11*, *16*). As described below, we consistently observed punctate fluorescence in several large buccal ganglion neurons and localized fluorescence on the R2 surface that formed a "fluorescent shell." Control experiments were performed by incubating ganglia in either artificial seawater (ASW) or DAF-2T ($N = 3$). In both experiments, none of the characteristic fluorescence described above was observed, indicating the probe must enter the membrane and the esters must be cleaved off before this fluorescence is observed.

Validation of NO Detection in *A. californica* Cells Using DAF-2 DA Incubation

Although reported to be specific (*28*, *29*), a concern when using this detection approach is that several other fluorescence products can be formed from DAF-2 reacting with other compounds, for example, dehydroascorbic acid (DHA). In addition, the reaction of DAF-2 with NO should be confirmed with chemically selective approaches, as described below. Moreover, the use of cell-permeable, acetate-based NO probes, such as DAF-2 DA, with *A. californica* cells needs to be well-validated.

To confirm that the fluorescence signal was from DAF-2T, we first verified esterase activity in the *A. californica* neurons. As shown in Figure 1b, when DAF-2 DA was incubated with the cell lysates from the *A. californica* CNS, DAF-2 was formed within 10 min, as confirmed by a DAF-2 peak observed using capillary electrophoresis−laser induced fluorescence (CE-LIF). A DAF-2 peak was also observed in the CE-LIF analysis of a single neuron dissected after DAF-2 DA incubation (Figure 2). In contrast, DAF-2 DA diluted into ASW showed little change (Figure 1b, trace 1). Furthermore, the cell lysate activity for converting DAF-2 DA to DAF-2 was tested after the tissue was boiled. The DAF-2 peak decreased to 50% when the cell lysate was placed in boiling water for 5 min and to 10% when the cell lysate was treated with three cycles of 10-s microwave irradiation following the boiling water bath. Since high temperature and microwave treatment are known to deactivate enzymes, these results suggest that the *A. californica* nervous system

DOI: 10.1021/cn900016z | *ACS Chem. Neurosci.* (2010), *1*, 182–193

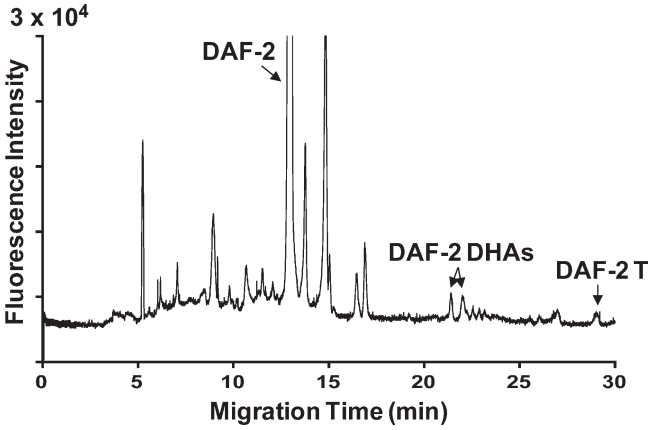

Figure 2. Representative electropherogram of an individual buccal neuron isolated after DAF-2 DA incubation. All of the labeled peaks were identified by comparison with standards run immediately before or after the CE assay and confirmed by sample spiking with standards. Note that DAF-2-DHAs were detected as a doublet peak because two reaction products were actually formed due to the conformational changes of DHA in solution.

possesses enzymes capable of converting DAF-2 DA into DAF-2.

Inside neurons, DAF-2 DA can be differentially accumulated into organelles, which maintain distinct pH levels. We investigated the influence of pH on the hydrolysis of acetate groups of DAF-2 DA in different buffer solutions (50 mM acetate buffer at pH 3.7, 0.1 M phosphate buffer at pH 7.4, 30 mM borate buffer at pH 9.8, and in ASW at pH 7.8). The extent of hydrolysis was monitored using CE-LIF. Specifically, the DAF-2T peak intensities of different solutions supplemented with DAF-2 or DAF-2 DA were compared. Some of these solutions were spiked with a known amount of NO. DAF-2 DA does not appreciably fluoresce at the excitation wavelength used by our CE-LIF system; thus, no DAF-2 DA peak was detected. However, DAF-2 and DAF-2T do fluoresce at this wavelength, and both were observed. CE separates these two compounds, so both can be quantified. It took 72 h under acidic conditions, 24 h under neutral pH conditions, and 3−5 min under basic conditions to observe the DAF-2 peak with CE-LIF. In ASW at pH 7.8, the hydrolysis was undetectable during a 1 h time period (Figure 1b, trace 1). In contrast, when DAF-2 DA was incubated with cell lysate from the *A. californica* CNS, DAF-2 formed within 10 min and was clearly observed in the electropherogram at a migration time of ~10 min (Figure 1b, trace 2).

Now that we know DAF-2 is found inside the cell, the next question is whether the fluorescence is from the reaction of DAF-2 with NO-related products. After all, DAF-2 reacts with other cellular constituents (*28*, *29*). Here we confirmed DAF-2T formation using both LC-MS and CE-LIF. These approaches serve to complement fluorescence imaging techniques by providing

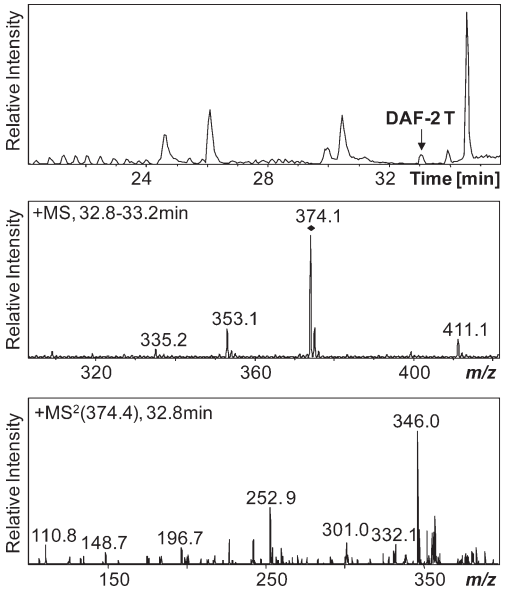

Figure 3. DAF-2T is detected with LC-MS in E-cluster homogenate after incubation with DAF-2 DA. Upper panel: Region of base peak chromatogram showing the retention time of DAF-2T. Middle panel: Region of the full MS spectrum showing the experimental m/z $(M+H)^+$ of 374.1, indicative of DAF-2T. Lower panel: MS/MS spectrum confirming the identity of DAF-2T signal.

chemical and structural information for the observed fluorescent product(s). As shown in Figure 3, DAF-2T was detected and confirmed using LC-MS from pooled E-cluster neurons, the best-studied NO-positive structure in *Aplysia* (*11*, *35*); the molecular mass and fragmentation pattern were matched to a DAF-2T standard. In the CE-LIF analysis, the identity of the DAF-2T peak was confirmed by comparing the migration time of the cellular constituents to a DAF-2T standard. Both analytical approaches confirmed that the fluorescence observed in *A. californica* neurons resulted from the presence of NO.

Previously, we reported an interfering effect on NO detection from intracellular DHA, which reacts with DAF-2. The reaction products, DAF-2 DHAs, fluoresce at the same emission wavelength as does DAF-2T (*29*, *36*). In the current work, during CE-LIF analysis, small DAF-2 DHA signals were observed, indicating that at least a small portion of the fluorescence comes from the reaction products of DAF-2 with intracellular DHA. DAF-2 DHAs were not observed with LC-MS, possibly because the instrument is not optimized for DAF-2 DHA detection. These results suggest that microseparations are necessary to differentiate NO-based fluorescence from other background fluorescence sources, or carefully designed pharmacological manipulations have to be performed to validate that the fluorescence originates from NO.

The presence of NOS in mechano/chemosensory C2 neurons in the E-clusters of *Aplysia* cerebral ganglia has

DOI: 10.1021/cn900016z | *ACS Chem. Neurosci.* (2010), *1*, 182–193

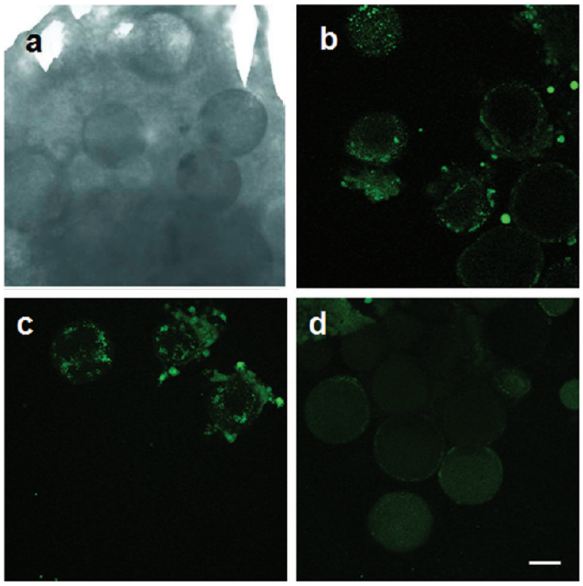

Figure 4. (a) Bright-field and (b) fluorescence from neurons in buccal ganglia incubated in ASW, (c) 1 mM L-arginine, and (d) 0.1 mM NOS inhibitor L-NAME, all treatments were done for 3 h before DAF-2 DA intracellular loading. All instrument settings for the images are the same. Scale bar = 50 μm.

been determined using several techniques (*11*, *35*). In our experiment, cerebral ganglion neurons were loaded with DAF-2 DA during 30-min incubation, subsequently rinsed with ASW, and then examined using fluorescence microscopy. Indeed, we observed fluorescence both in the neuropil and in several E-cluster cells. To confirm that the fluorescence was related to the product of a reaction between DAF-2 and NO, the neuropil and E-clusters were dissected and homogenized in 5 uL of phosphate buffer. After centrifugation at 10,000 × g for 5 min, the supernatant was analyzed using LC-MS (Figure 3) and CE-LIF (data not shown). As shown in Figure 3, the DAF-2T peak appeared at the retention time of 33 min. The monoisotopic mass (observed mass, 374.1 Da, mass error, 27 ppm) and tandem MS (MS/MS) fragmentation pattern match those of DAF-2T standard. The DAF-2T peak was also observed with CE-LIF. Thus, the fluorescence is confirmed to be from the reaction of DAF-2 and NO.

NO Production in Buccal Neurons

Once the detection of NO was verified in the known NOS-positive cerebral E-cluster, buccal ganglion neurons were examined ($N > 5$). Figure 4 shows punctate fluorescence, 1.5 ± 0.7 μm in diameter (mean ± SD), seen in the buccal neurons. Laser scanning at different depths (Z-axis profiling) confirmed that the fluorescence arises from inside the neurons (Figure S2, Supporting Information). To demonstrate that the NO is generated by NOS, buccal ganglia were incubated in the NOS substrate L-arginine or NOS inhibitor L-NAME. Cell boundaries were outlined according to the best judgment of the observer during evaluation of the number and intensity of fluorescent puncta. The average brightness of a single cell was determined as the ratio of the mean pixel value in the cell boundary over the background level. The average number of puncta was estimated by comparing the percentage of pixels in the cell boundary having a value more than 10 times higher than the background level. When the buccal ganglia were preincubated with L-arginine for 3 h before DAF-2 DA loading, the fluorescence intensity did not increase (the mean intensity of buccal neurons is 4.7 ± 0.8, the mean intensity of buccal neurons in arginine incubation is 5.1 ± 0.1, $P = 0.42$, $N = 3$) but more points appeared (Figure 4c, 14.0% ± 1.0% of total pixels has a value greater than 10 times the background level in buccal neurons with arginine incubation but only 10.0% ± 3.1% in buccal neurons with ASW incubation, $P = 0.05$, $N = 3$). With preincubation by the NOS inhibitor L-NAME, the strongly fluorescent puncta disappeared (Figure 4d, $P < 0.001$, $N = 5$). These experiments suggest that the studied neurons express NOS-like enzymes and the observed puncta are related to NO.

We next confirmed that some of the fluorescence was from DAF-2T, the reaction product of NO with DAF-2. In previous experiments (*28*, *29*, *36*), single-cell NO detection was carried out by first dissecting the *A. californica* neurons and then reacting the cell contents with DAF-2 *in vitro*. Interestingly, in that experimental paradigm, DAF-2T was rarely observed. This may be because NO dissipates and little or no new NO is generated during this several minutes long sample preparation process. Therefore, to minimize the possibility that NO production is altered by the single-cell isolation and homogenization procedures, intact buccal ganglia were quickly desheathed and incubated in DAF-2 DA solutions without further cell isolation. After incubation, individual *A. californica* neurons with intense fluorescence were isolated and analyzed with CE-LIF. Specifically, the buccal neurons that became fluorescent after incubation with DAF-2 DA were isolated and studied (Figure 2). The DAF-2 peak was observed in these cells, indicating DAF-2 DA is indeed converted to DAF-2. Further, the DAF-2T peak (and the peaks from the reaction products between DAF-2 and DHA, DAF-2 DHAs) is also present in the electropherograms. As shown in Figure 2, the intensity of the DAF-2T peak and the signal-to-background noise ratio, as well as results of our pharmacological experiments described above, are sufficient to confirm the presence of NO in these cells. However, the NO concentration in these cells is close to the CE system detection limit, in part due to the need to dilute single-cell samples to allow sample injection into the CE separation capillary. Because of

DOI: 10.1021/cn900016z | *ACS Chem. Neurosci.* (2010), *1*, 182–193

these low levels, further biochemical studies were not undertaken.

There are about 20 motor neurons located on the surface of the buccal ganglia that regulate the movement of the feeding apparatus, comprised of eight intrinsic muscles (*37*, *38*). The release of several classical and peptide neurotransmitters and neuromodulators by some of these neurons has been reported (*39*, *40*). In our DAF-2 DA incubation experiments, many of the larger neurons consistently showed internal fluorescence. The intensity of this fluorescence was modulated by pharmacological treatment of cells with NOS substrate or NOS inhibitor and, as shown by CE-LIF analysis, in part attributed to DAF-2T. These findings are in good agreement with the well-recognized role of NO in feeding behavior (*41*).

Interestingly, the distribution of the NO fluorescence that we observed in the buccal neurons is not homogeneous but punctate. Several questions can be asked about the origin of these fluorescence puncta. Are these puncta observed because NO production is discretely localized? Is DAF-2 DA, after passing across the cell membrane, confined to restricted locations such as organelles or protein aggregates? Does punctate fluorescence reflect NO dynamics? NOS association with subcellular organelles has been reported in mammalian cells; the endoplasmic reticulum, nuclear envelope, Golgi apparatus, and mitochondrial membrane are such structures (*42*, *43*). However, little evidence of the subcellular distribution of NOS has been reported in molluscan species. Assuming that *A. californica* NOS is localized as indicated in mammalian studies, after NO generation, NO would diffuse in all directions and react with various cellular components. As shown in the supplemental calculations and assuming Fick's second law of diffusion, the NO source should be at least several micrometers in diameter, and this would spread after NO generation as the DAF-2T diffused throughout the cytoplasm. The punctate nature of fluorescence indicates that the fluorescent dye is likely sequestered in subcellular organelles

Another interesting observation is that the brightness of the fluorescence puncta far surpasses the fluorescence intensity seen in the *in vitro* reaction of 10 μM DAF-2 with 2 mM NO, the saturating level in aqueous solution, prepared by passing NO through the phosphate-buffered saline solution. A possible explanation for this may be that with the incubation conditions commonly used (10 μM DAF-2 DA), DAF-2 accumulates intracellularly to the millimolar range (*44*). Thus, the puncta may be as bright as they are because they accumulate probe. Due to the possible DAF-2 accumulation, NO quantification is a difficult task in living cells. In this case, the average concentration of DAF-2T, which reflects NO concentration, has to be determined by other methods such as CE-LIF.

NO in Abdominal Ganglion R2 and Bag Cell Neurons

The puncta localization is cell specific. By the same approach described above, intense fluorescence was observed on the surface of several neurons but not intracellularly. The most prominent of these neurons is the well-known cholinergic R2 neuron in the abdominal ganglion of *A. californica*. The R2 is the largest neuron in *Aplysia* (*45*) and its axon runs unbranched in the right pleuroabdominal connective, ultimately to synapse on glands in the animal's skin. It has been extensively studied as a model for regional protein and lipid syntheses and their axonal transportation. The R2 is easily identified visually in the desheathed abdominal ganglion. Intriguingly, NO-related fluorescence is detected in the R2 neuron, but in this case, it was localized on the R2 surface, forming a "fluorescent shell" ($N = 3$, Figure 5). A 20-μm step depth scan of the neuron revealed an absence of fluorescent signal from inside the cell. It is intriguing that in the abdominal ganglion, only a few neurons demonstrated this form of fluorescence, making it less likely this is a sampling artifact. As mentioned previously, neither DAF-2T nor ASW preincubation produced fluorescence of these structures under these conditions.

One possible explanation for the fluorescence shell seen in the R2 neurons is that the fluorescence results from NO production in the glia embracing the R2 cell body. It is known that giant *Aplysia* neurons such as the R2 are surrounded by numerous glia interspersed by extracellular space and forming thin concentric layers (*46*−*48*). Microstructural analysis of the abdominal ganglion in a semi-intact preparation by scanning electron microscopy (SEM) (Figure 5d, e) revealed that the R2 surface exhibits substantial roughness. Details of the surface microstructure observed by SEM were comparable to what we observed with the confocal microscope. Membrane roughness has been previously reported as especially extensive in giant neurons (*49*, *50*). The origin of these dense mesh-like structures made of thin fibers covering the surface of the R2 neuron and adjacent neurons are unknown but may be neuronal terminals, glia, or other structures. This roughness could also in part be a laminar material from extracellular matrix or connective sheath remnants that have been infiltrated by neuronal and glia terminals. Regardless, our SEM analysis did not reveal the presence of distinct glia on the surface of the R2 neuron, suggesting that the protease treatment used in this study prior to desheathing of the ganglia may promote glia removal. Disruption of glia cohesion, and even their complete elimination by protease and mechanical treatments, has been reported

DOI: 10.1021/cn900016z | *ACS Chem. Neurosci.* (2010), *1*, 182–193

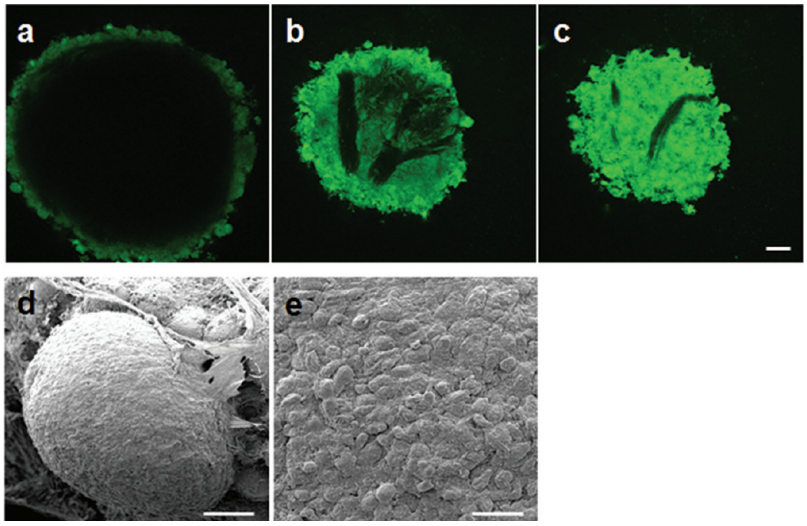

Figure 5. Fluorescence of an R2 neuron after DAF-DA exposure. (a-c) Confocal fluorescence images of a R2 neuron at different depths of Z-axis scans showing the fluorescence localized on the R2 surface. Scale bar = 50 μm. (d, e) Scanning electron microscopy of a R2 neuron surface at different magnification levels. Scale bar in (d) = 50 μm. Scale bar in (e) = 12.5 μm.

in earlier morphology studies of desheathed R2 neurons for electron microscopy (*47*).

It is also possible that the observed fluorescence is partially from neurite terminals infiltrating the surrounding extracellular matrix and targeting the R2 neuron. It has been reported that NOS is present at the neuronal synapse (*51*). Our previous study also suggested NO production at the tip of the neuronal growth cone (*26*). To determine whether neuronal terminals can produce NO, we used the easy-to-culture abdominal bag cell neurons and then determined the NO production at their terminals. Cultured bag cells form growth cones and elaborate extended neurites. Some of these neurites can measure up to 20-μm across at their tips and 60-μm long. Indeed, we observed strong NO-related fluorescence at the tips of these terminals, as shown in Figure 6. One can envision a scenario in which the oxidative stress caused by mechanical disruptions and imaging of the cells, coupled with DAF-2 reacting with peroxynitrite (*52*), is responsible for some of the fluorescence. Thus the cultured cells, along with their terminals, were collected and analyzed by CE-LIF. Additionally, five cultured bag cell neurons were pooled together and analyzed using LC-MS. Both techniques confirmed the presence of DAF-2T (and hence genuine NO) in the terminals (data not shown). These results suggest that NO is produced at *A. californica* neuronal terminals *in vitro*. Considering that an increasing number of reports suggest that NO is an important regulator of neurite outgrowth and growth cone motility (for review, see ref (*53*)), it is logical to speculate that the fluorescence observed on the surface of the R2 may result from the NO-producing neuronal terminals popu-

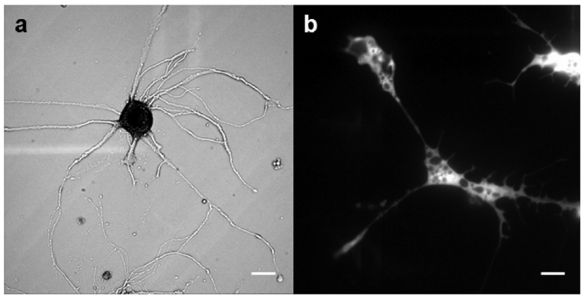

Figure 6. DAF-2DA incubation of cultured bag cell neurons results in NO-related fluorescence localized in neurites. (a) Bright-field image of cultured bag cell neurons from abdominal ganglia. Scale bar = 50 μm. (b) Fluorescence image of fine neurites and growth cones extending from a cultured bag cell. Scale bar = 20 μm.

lating the R2 surface. However, glia and their processes on the R2 exterior cannot be excluded as potential sources of the observed fluorescence.

Both the fluorescence at the R2 surface and at the terminals of cultured bag cell neurons are pharmacologically different from the fluorescence developed in the buccal cells. The formation of fluorescent signal on the R2 surface after incubation with DAF-2 DA was not prevented by preincubation with the NOS inhibitor L-NAME at various concentrations, ranging from the conventionally used 0.1 mM (average decrease of signal intensity, 0.7% ± 3.0%, N = 3) to the highest dose of 10 mM (average increase, 5.7% ± 4.5%, N = 3). Incubations of the NOS substrate L-arginine, or NO-generating pathway products such as L-citrulline and L-argininosuccinate, also had no effect on the intensity of the fluorescent signal in the "shell" (intensity change within 5% as compared to a control experiment, N = 3). These experiments were also repeated with cultured bag cell

DOI: 10.1021/cn900016z | *ACS Chem. Neurosci.* (2010), *1*, 182–193

neurons. As with the R2 neuron experiments, no significant differences were observed in the fluorescence intensities at the bag cell neurite terminals at the above-mentioned conditions. These results are puzzling in that NO generated by known forms of NOS and the fluorescence from the buccal neurons are affected by these factors. CE-LIF and MS results demonstrated DAF-2T in these cells. Therefore the fluorescence is, at least in part, NO-related.

These results may be explained by the presence of a NOS-like enzyme with a unique pharmacology, the production of NO without an enzyme, or perhaps an artifact caused by the cell manipulations and microscope illumination. An experimental artifact appears less likely because the distinct NO sources are location specific and have been confirmed via CE-LIF and MS. Enzyme-independent NO production has been proposed to explain results of experiments where a high concentration of L-NAME was found unable to suppress NO production in the presence of NADPH, glutathione, L-cysteine, dithiothreitol or ascorbate (*54*). In this case, nitrite reduction to NO in an acidic environment is suggested as an alternative pathway to enzymatic NO production. Molluscan neurons have high concentrations (millimolar levels in some cases) of nitrite (*55*−*57*). The neurite terminals contain numerous large, dense-core vesicles (*58*). The pH inside these vesicles is more acidic than the cytoplasmic environment, possibly enhancing NO formation from nitrite. While further experiments are underway to investigate this phenomenon, the present results have important implications for understanding NO production.

In conclusion, we performed NO fluorescence imaging after whole ganglion incubation with DAF-2 DA, thereby minimizing neuronal damage, abnormal NO redistribution, and artificial NO removal by scavenging molecules. Using these methods, we verified NO production in several *A. californica* neurons by confocal microscopy, CE, MS, and pharmacological tools. Intriguingly, the punctuate fluorescence found in several buccal neurons responds to known NOS pharmacological treatments, while the surface-based fluorescence detected in the R2 neuron and bag cell neuron terminals is not affected by NOS inhibitors. The sequencing and annotation of the *A. californica* genome is well underway (*59*); it will be interesting to determine whether unusual NOS genes are encoded in that genome.

Methods

Chemicals and Reagents

All reagents were of high purity and were obtained from Sigma-Aldrich (St. Louis, MO) unless otherwise noted. The CE buffer, 30 mM sodium borate, contained 0.03 g of boric acid (H_3BO_3) and 0.97 g of sodium borate decahydrate ($Na_2B_4O_7 \cdot 10H_2O$) in 100 mL of ultrapure water (Millipore, Bedford, MA), adjusted to pH 9.85 ± 0.05 with 3 M NaOH (Fisher Scientific, Fair Lawn, NJ). The 0.1 M phosphate buffer (pH 7.4 ± 0.1) was prepared using 0.26 g of monobasic sodium phosphate ($NaH_2PO_4 \cdot H_2O$) and 2.17 g of dibasic sodium phosphate ($Na_2HPO_4 \cdot 7H_2O$) in 100 mL of ultrapure water. DAF-2 and DAF-2 DA were purchased from EMD Biosciences, Inc. (Calbiochem, La Jolla, CA). The original fluorescent reagents, dissolved in dimethyl sulfoxide (DMSO), were diluted into the desired buffer. The final concentration of DMSO in the DAF-2 and DAF-DA solutions was less than 1% (v/v). NO gas with 99% purity was obtained from Matheson Gas (through S. J. Smith Welding Supply, Urbana, IL). To prepare the NO-saturated solution, a 0.1 M phosphate buffer solution (pH 7.4) was deoxygenated with nitrogen for 20 min and then bubbled with NO gas previously cleaned by passing through 5 M NaOH solution. The saturated solution contains ∼1.9 mM NO at room temperature.

Sample Preparation

Aplysia californica (100−200 g) were obtained from the Aplysia Research Facility (University of Miami, Miami, FL) and kept in an aquarium containing continuously circulating, aerated, and filtered in-house prepared seawater at 14−15 °C until needed. Animals were anesthetized by injection of isotonic $MgCl_2$ (∼30 to ∼50% of body weight) into the body cavity. The cerebral, buccal, and abdominal ganglia were dissected and placed in artificial seawater (ASW) containing (in mM) 460 NaCl, 10 KCl, 10 $CaCl_2$, 22 $MgCl_2$, 6 $MgSO_4$, and 10 HEPES, pH 7.7. The ganglionic sheath was digested enzymatically by incubating the ganglia in ASW containing 10 mg/mL protease IX and 10 mg/mL protease XIV (bacterial; Sigma-Aldrich) at 34 °C for 30 min. After the ganglia were washed in fresh ASW, the connective tissue sheath surrounding the neurons was removed mechanically. The ganglia were immediately transferred into glass vials containing 10 μM of DAF-2 DA solution and incubated for 15 min at 14 °C for dye loading. After incubation, the ganglia were either directly mounted onto a fluorescence microscope for imaging or further prepared for cellular analysis. Identified neurons and neuronal clusters designated for cellular investigation were manually dissected using sharp tungsten needles or microscissors and transferred with ∼1 μL of ASW into small plastic tubes (Costar, Corning, NY) for analysis via CE-LIF or LC-MS.

Cell Culture

Bag cell neurons (10−20) from the abdominal ganglia were isolated and distributed on poly(L-lysine)-coated Nunc Lab-Tek chambered borosilicate cover glasses (Fisher Scientific). The culture medium consisted of ASW enriched with 0.1 mg/mL methionine, 0.3 mg/mL glutamate, and 1.1 mg/mL glucose. Culture dishes were not moved for 1 h after seeding to allow cells to settle and were kept for 2 d at 15 °C before performing fluorescence imaging.

Microinjection and Cellular Recordings

A. californica neurons were manually pressure-injected through glass microelectrodes filled with 10 μM or 2 mM DAF-2 in intracellular solution (in mM): 506 mM KCl, 5 mM HEPES, titrated with KOH to pH 7.7, supplemented with 5 mg/mL green triarylmethane dye (fast green FCF) and variable amounts of DMSO present in DAF-2 stock solution. A Leica MZ75 stereomicroscope (Leica Microsystems GmbH,

DOI: 10.1021/cn900016z | *ACS Chem. Neurosci.* (2010), *1*, 182–193

Wetzlar, Germany) allowed visual control of the volume of solution injected. The health of the injected cells before, during, and after injection was electrophysiologically monitored in current clamp mode using a system comprised of an AxoClamp 2B amplifier, a Digidata, 1322A D/A−A/D converter, the software package pClamp 9 (all from Molecular Devices, Sunnyvale, CA) and a computer. Green-colored neurons exhibiting normal membrane potentials and excitability after injection were considered successfully loaded with DAF-2. Control injections of the intracellular solution containing similar amounts of DMSO to ones used in the experiments with DAF-2 injections were done to determine the possible effects of the compounds loaded into neurons on the electrophysiological parameters of the cell. No adverse effects were observed.

Hydrolysis of DAF-2 DA by *A. californica* Central Nervous System Homogenate

The *A. californica* cerebral and buccal ganglia were dissected and desheathed as described above. Individual ganglia were homogenized with a 5-fold excess (by weight) of tris-HCl buffer (0.1 M, pH 7.6) prepared in ASW containing 0.1% Triton X-100 followed by three cycles of 5 s sonication. The homogenate was centrifuged at 14000 rpm at 14 °C for 10 min to remove larger pieces of cell membrane and sheath material. The supernatant was divided into three 5-μL aliquots and tested for DAF-2 DA hydrolysis under three different conditions. The first aliquot was mixed with 5 μL of 20 μM DAF-2 DA and incubated at 14 °C for 10 min. The second aliquot was bathed in boiling water for 5 min before incubation with DAF-2 DA. The third aliquot was first water bathed and then microwaved for three cycles of 10 s each.

Fluorescence Microscopy

Bright-field and fluorescence micrographs were obtained by a Zeiss Axiovert 200 M inverted microscope (Carl Zeiss MicroImaging, Standort Gottingen, Germany) using a halogen lamp (100 W) and an Hg lamp (150 W) as light sources. Images were acquired via an EMCCD camera (Cascade 512B; Roper Scientific, Tucson, AZ). The entire system was driven using Zeiss Axiovision, a software package that facilitates image collection. Both 40× and a 63× (oil) objective lenses were used. A Leica SP2 confocal laser scanning microscope (Leica Microsystems) with a 40× (oil) objective lens and Ar^+ laser (488 nm) excitation source was employed for high resolution fluorescence imaging. A long-pass filter (λ > 515 nm) was used to remove reflected light and to measure fluorescence. Automatic in-depth scanning was performed using a Z-scan motor, which changes the position of the objective along the Z-axis. The top focal plane of the neuron of interest was set as the beginning scan plane. The working distance and step size were set to 100 and 10 μm, respectively. All pictures presented herein are unprocessed.

CE-LIF

The CE system employed in this work has been described in detail elsewhere (*60*, *61*). Briefly, a laboratory-assembled CE system, consisting of an Ar/Kr mixed gas laser (Innova 70 Spectrum; Coherent, Inc., Palo Alto, CA) producing 350−356 nm of excitation light, a photomultiplier tube (PMT) (HC125-03; Hamamatsu, Bridgewater, NJ), and an 80-cm long, 50-μm inner diameter fused silica capillary (Polymicro Technologies, Phoenix, AZ), was employed for separation and monitoring of the reaction products of DAF-2 with NO and with other compounds. Injections took place at 8 kV (12 μA) for 8 s, corresponding to a 7.6 nL injection volume. Separations were performed at 20 kV (40−42 μA). Detection took place on-capillary, 60 cm beyond the point of injection. The fluorescence was collected at 90° by an all-reflective microscope objective (Ealing Electro-Optical, Holliston, MA) and filtered spatially by a machined 3 mm pinhole and spectrally by an 80 nm fwhm, 500 nm interference filter (03FIB004; Melles Griot, Irvine, CA) and a high-pass filter (400EFLP; Janos Technology, Townshend, VT). The PMT signal, consisting of a series of TTL pulses, was processed using a data acquisition card (6024E; National Instruments, Austin, TX); all counting, instrumentation, and voltages were controlled by a custom-tailored program written in Labview (version 5.0.1; National Instruments).

LC-MS

Both the E-cluster homogenate, after DAF-2 DA incubation, and the DAF-2T standard, prepared by blowing NO gas into the DAF-2 solution for 5 min, were subjected to LC-MS analyses. For each sample, 5 μL of solution was purified using capillary LC (capLC, Waters, Milford, MA), equipped with a C18 Pepmap column (150 × 0.3 mm inner diameter) packed with 3 μm diameter 100 Å pore-size particles (Dionex, Sunnyvale, CA) at a flow rate of 2.5 μL/min. Solvents A and B consisted of 0.1% acetic acid/0.01% trifluoroacetic acid (TFA) (v/v) and 99.91% CH_3CN/0.08% acetic acid/0.01% TFA (v/v), respectively. A six-step linear gradient was used (0−20% B in 10 min; 20−40% B in 15 min; 40−80% B in 5 min; 80−80% B in 3 min; 80−20% B in 2 min; 20−10% B in 5 min). The eluent was directly interfaced to an electrospray mass spectrometer (HCTultra PTM Discovery System; Bruker Daltonics, Bremen, Germany) for characterization. The MS data were acquired over a range of 300−700 m/z, and MS/MS data were obtained automatically in a data-dependent acquisition mode.

Scanning Electron Microscopy (SEM) of R2 Neurons

Isolated abdominal ganglia were first subjected to protease treatment (1% protease type IX) in ASW-antibiotic solution (ASW containing 100 units/mL penicillin G, 100 μg/mL streptomycin, and 100 μg/mL gentamicin, pH 7.7) at 34 °C for 1 h, and then washed for 3 h in ASW. The connective tissue was partially removed to expose the neurons of interest. Mounted dorsal side up onto a SYLGARD 184 silicone elastomer surface (Dow Corning, Midland, MI), ganglia were fixed with modified Karnovsky's fixative (2% glutaraldehyde/2% paraformaldehyde in 0.1 M phosphate buffer) for 4 h at 4 °C. After being washed with phosphate buffer for at least 30 min, specimens were briefly rinsed with distilled water and dehydrated in a series of graded ethyl alcohol solutions, 15 min each: 33%, 67%, 95%, and two changes of 100%. Dehydrated specimens were transferred into Teflon porous vials and processed for critical point drying using the Samdri-PVT-3D drier (Tousimis, Rockville, MD). For SEM imaging, a 5-nm coat of palladium/gold was deposited onto the dried specimens using a sputter coater. Samples were viewed using a Philips XL30 ESEM-FEG microscope (FEI Company, Hillsboro, OR). All images are unprocessed.

DOI: 10.1021/cn900016z | *ACS Chem. Neurosci.* (2010), *1*, 182–193

Supporting Information Available

The Supporting Information includes bright-field and fluorescence micrographs of the cerebral ganglion after DAF-2 DA incubation (Figure S1), serial Z-stack images of an individual buccal neuron (Figure S2) and discussion and a plot of the spatial distribution of NO as it diffuses, calculated by Fick's second law of diffusion (Figure S3). This material is available free of charge via the Internet at http://pubs.acs.org.

Author Information

Corresponding Author

*Mailing address: Department of Chemistry, University of Illinois, 600 South Mathews Ave. 63-5, Urbana, IL; 61801. E-mail: jsweedle@illinois.edu.

Author Contributions

X.Y., S.S.R, and J.V.S. designed the research; X.Y. performed the capillary electrophoresis and fluorescence microscopy; F.X. was responsible for the mass spectrometry; E.V. R performed the electron microscopy; S.S.R. did cell isolation, physiology, and culturing; X.Y., E.V.R., S.S.R, and J.V.S. analyzed the data; X.Y., E.V.R., S.S.R, and J.V.S. wrote the paper.

Funding Sources

The project described was supported by Award Number P30 DA018310 from the National Institute On Drug Abuse (NIDA), and the National Institute of Neurological Disorders and Stroke (NINDS) by Award No. NS031609. The content is solely the responsibility of the authors and does not necessarily represent the official views of the NIDA, NINDS, or the National Institutes of Health. The SEM located in the Beckman Institutes Microscopy Suite was partially purchased from funds from the National Science Foundation Award No. DBI-9871103.

Acknowledgment

The authors gratefully thank Jonathan Ekman and Duohai Pan for assisting with the confocal fluorescence microscope and Scott Robinson for his assistance with SEM.

Abbreviations

ASW, artificial seawater; CE, capillary electrophoresis; CE-LIF, capillary electrophoresis−laser induced fluorescence; CNS, central nervous system; DAF-2 DA, 4,5-diaminofluorescein diacetate; DAF-2, 4,5-diaminofluorescein; DHA, dehydroascorbic acid; DMSO, dimethyl sulfoxide; HEPES, *N*-2-hydroxyethylpiperazine-*N*′-2ethanesulfonic acid; LC-MS, liquid chromatography mass spectrometry; L-NAME, L-nitro-arginine methyl ester; MS, mass spectrometry; NADPH-d, NADPH-diaphorase; NO, nitric oxide; NOS, NO synthases; SEM, scanning electron microscopy; TFA, trifluoroacetic acid; TTL, transistor−transistor logic.

References

1. Garthwaite, J., and Boulton, C. L. (1995) Nitric oxide signaling in the central nervous system. *Annu. Rev. Physiol. 57*, 683–706.

2. Holscher, C. (1997) Nitric oxide, the enigmatic neuronal messenger: Its role in synaptic plasticity. *Trends Neurosci. 20*, 298–303.

3. Meffert, M. K., Calakos, N. C., Scheller, R. H., and Schulman, H. (1996) Nitric oxide modulates synaptic vesicle docking fusion reactions. *Neuron 16*, 1229–1236.

4. Schuman, E. M., and Madison, D. V. (1994) Nitric oxide and synaptic function. *Annu. Rev. Neurosci. 17*, 153–183.

5. Bredt, D. S., and Snyder, S. H. (1992) Nitric oxide, a novel neuronal messenger. *Neuron 8*, 3–11.

6. Bredt, D. S., and Snyder, S. H. (1994) Nitric oxide: A physiologic messenger molecule. *Annu. Rev. Biochem. 63*, 175–195.

7. Snyder, S. H., and Ferris, C. D. (2000) Novel neurotransmitters and their neuropsychiatric relevance. *Am. J. Psychiatry 157*, 1738–1751.

8. Bredt, D. S., Glatt, C. E., Hwang, P. M., Fotuhi, M., Dawson, T. M., and Snyder, S. H. (1991) Nitric oxide synthase protein and mRNA are discretely localized in neuronal populations of the mammalian CNS together with NADPH diaphorase. *Neuron 7*, 615–624.

9. Iwase, K., Iyama, K., Akagi, K., Yano, S., Fukunaga, K., Miyamoto, E., Mori, M., and Takiguchi, M. (1998) Precise distribution of neuronal nitric oxide synthase mRNA in the rat brain revealed by non-radioisotopic in situ hybridization. *Mol. Brain Res. 53*, 1–12.

10. Kandel, E. R. (2001) The molecular biology of memory storage: A dialogue between genes and synapses. *Science 294*, 1030–1038.

11. Jacklet, J. W. (1995) Nitric oxide is used as an orthograde cotransmitter at identified histaminergic synapses. *J. Neurophysiol. 74*, 891–895.

12. Elphick, M. R., Kemenes, G., Staras, K., and O'Shea, M. (1995) Behavioral role for nitric oxide in chemosensory activation of feeding in a mollusc. *J. Neurosci. 15*, 7653–7664.

13. Teyke, T. (1996) Nitric oxide, but not serotonin, is involved in acquisition of food-attraction conditioning in the snail *Helix pomatia*. *Neurosci. Lett. 206*, 29–32.

14. Korneev, S. A., Piper, M. R., Picot, J., Phillips, R., Korneeva, E. I., and O'Shea, M. (1998) Molecular characterization of NOS in a mollusc: Expression in a giant modulatory neuron. *J. Neurobiol. 35*, 65–76.

15. Jacklet, J. W., and Gruhn, M. (1994) Co-localization of NADPH-diaphorase and myomodulin in synaptic glomeruli of *Aplysia*. *Neuroreport 5*, 1841–1844.

16. Moroz, L. L. (2006) Localization of putative nitrergic neurons in peripheral chemosensory areas and the central nervous system of *Aplysia californica*. *J. Comp. Neurol. 495*, 10–20.

17. Moroz, L. L., and Gillette, R. (1996) NADPH-diaphorase localization in the CNS and peripheral tissues of the

DOI: 10.1021/cn900016z | *ACS Chem. Neurosci.* (2010), *1*, 182–193

predatory sea-slug *Pleurobranchaea californica*. *J. Comp. Neurol. 367*, 607–622.

18. Moroz, L. L., Gillette, R., and Sweedler, J. V. (1999) Single-cell analyses of nitrergic neurons in simple nervous systems. *J. Exp. Biol. 202*, 333–341.

19. Yang, Q., Zhang, X., Bao, X., Lu, H., Zhang, W., Wu, W., Miao, H., and Jiao, B. (2008) Single cell determination of nitric oxide release using capillary electrophoresis with laser-induced fluorescence detection. *J. Chromatogr. A 1201*, 120–127.

20. Lee, Y., Oh, B. K., and Meyerhoff, M. E. (2004) Improved planar amperometric nitric oxide sensor based on platinized platinum anode. 1. Experimental results and theory when applied for monitoring NO release from diazeniumdiolate-doped polymeric films. *Anal. Chem. 76*, 536–544.

21. Patel, B. A., Arundell, M., Parker, K. H., Yeoman, M. S., and O'Hare, D. (2006) Detection of nitric oxide release from single neurons in the pond snail, *Lymnaea stagnalis*. *Anal. Chem. 78*, 7643–7648.

22. Brown, F. O., and Lowry, J. P. (2003) Microelectrochemical sensors for in vivo brain analysis: An investigation of procedures for modifying Pt electrodes using Nafion. *Analyst 128*, 700–705.

23. Kojima, H., Hirotani, M., Nakatsubo, N., Kikuchi, K., Urano, Y., Higuchi, T., Hirata, Y., and Nagano, T. (2001) Bioimaging of nitric oxide with fluorescent indicators based on the rhodamine chromophore. *Anal. Chem. 73*, 1967–1973.

24. Kojima, H., Nakatsubo, N., Kikuchi, K., Kawahara, S., Kirino, Y., Nagoshi, H., Hirata, Y., and Nagano, T. (1998) Detection and imaging of nitric oxide with novel fluorescent indicators: Diaminofluoresceins. *Anal. Chem. 70*, 2446–2453.

25. Sato, M., Nakajima, T., Goto, M., and Umezawa, Y. (2006) Cell-based indicator to visualize picomolar dynamics of nitric oxide release from living cells. *Anal. Chem. 78*, 8175–8182.

26. Ye, X., Rubakhin, S. S., and Sweedler, J. V. (2008) Simultaneous nitric oxide and dehydroascorbic acid imaging by combining diaminofluoresceins and diaminorhodamines. *J. Neurosci. Methods 168*, 373–382.

27. Kim, W. S., Ye, X., Rubakhin, S. S., and Sweedler, J. V. (2006) Measuring nitric oxide in single neurons by capillary electrophoresis with laser-induced fluorescence: Use of ascorbate oxidase in diaminofluorescein measurements. *Anal. Chem. 78*, 1859–1865.

28. Ye, X., Rubakhin, S. S., and Sweedler, J. V. (2008) Detection of nitric oxide in single cells. *Analyst 133*, 423–433.

29. Zhang, X., Kim, W. S., Hatcher, N., Potgieter, K., Moroz, L. L., Gillette, R., and Sweedler, J. V. (2002) Interfering with nitric oxide measurements. 4,5-diaminofluorescein reacts with dehydroascorbic acid and ascorbic acid. *J. Biol. Chem. 277*, 48472–48478.

30. Grynkiewicz, G., Poenie, M., and Tsien, R. Y. (1985) A new generation of Ca2+ indicators with greatly improved fluorescence properties. *J. Biol. Chem. 260*, 3440–3450.

31. Williams, D. A., Fogarty, K. E., Tsien, R. Y., and Fay, F. S. (1985) Calcium gradients in single smooth muscle cells revealed by the digital imaging microscope using Fura-2. *Nature 318*, 558–561.

32. Wertz, A., Rossler, W., Obermayer, M., and Bickmeyer, U. (2006) Functional neuroanatomy of the rhinophore of *Aplysia* punctata. *Front. Zool. 3*, 6.

33. Herring, T. L., Slotin, I. M., Baltz, J. M., and Morris, C. E. (1998) Neuronal swelling and surface area regulation: Elevated intracellular calcium is not a requirement. *Am. J. Physiol. 274*, C272–281.

34. Michel, S., Ehnert, C., and Schildberger, K. (2002) FMRFamide modulates potassium currents in circadian pacemaker neurons of *Bulla gouldiana*. *Neuroscience 110*, 181–190.

35. Jacklet, J., Grizzaffi, J., and Tieman, D. (2004) Serotonin, nitric oxide and histamine enhance the excitability of neuron MCC by diverse mechanisms. *Acta Biol. Hung. 55*, 201–210.

36. Ye, X., Kim, W. S., Rubakhin, S. S., and Sweedler, J. V. (2004) Measurement of nitric oxide by 4,5-diaminofluorescein without interferences. *Analyst 129*, 1200–1205.

37. Church, P. J., and Lloyd, P. E. (1994) Activity of multiple identified motor neurons recorded intracellularly during evoked feedinglike motor programs in *Aplysia*. *J. Neurophysiol. 72*, 1794–1809.

38. Scott, M. L., Govind, C. K., and Kirk, M. D. (1991) Neuromuscular organization of the buccal system in *Aplysia californica*. *J. Comp. Neurol. 312*, 207–222.

39. Church, P. J., Whim, M. D., and Lloyd, P. E. (1993) Modulation of neuromuscular transmission by conventional and peptide transmitters released from excitatory and inhibitory motor neurons in *Aplysia*. *J. Neurosci. 13*, 2790–2800.

40. Weiss, K. R., Brezina, V., Cropper, E. C., Hooper, S. L., Miller, M. W., Probst, W. C., Vilim, F. S., and Kupfermann, I. (1992) Peptidergic co-transmission in *Aplysia*: Functional implications for rhythmic behaviors. *Experientia 48*, 456–463.

41. Katzoff, A., Ben-Gedalya, T., Hurwitz, I., Miller, N., Susswein, Y. Z., and Susswein, A. J. (2006) Nitric oxide signals that *Aplysia* have attempted to eat, a necessary component of memory formation after learning that food is inedible. *J. Neurophysiol. 96*, 1247–1257.

42. Gonzalez-Hernandez, T., Perez de la Cruz, M. A., and Mantolan-Sarmiento, B. (1996) Histochemical and immunohistochemical detection of neurons that produce nitric oxide: Effect of different fixative parameters and immunoreactivity against non-neuronal NOS antisera. *J. Histochem. Cytochem. 44*, 1399–1413.

43. Hecker, M., Mulsch, A., and Busse, R. (1994) Subcellular localization and characterization of neuronal nitric oxide synthase. *J. Neurochem. 62*, 1524–1529.

44. Rodriguez, J., Specian, V., Maloney, R., Jourd'heuil, D., and Feelisch, M. (2005) Performance of diamino fluorophores for the localization of sources and targets of nitric oxide. *Free Radical Biol. Med. 38*, 356–368.

45. Lovell, P., Jezzini, S. H., and Moroz, L. L. (2006) Electroporation of neurons and growth cones in *Aplysia californica*. *J. Neurosci. Methods 151*, 114–120.

46. Keicher, E., Bilbaut, A., Maggio, K., Hernandez-Nicaise, M. L., and Nicaise, G. (1991) The desheathed periphery of *Aplysia* giant neuron. Fine structure and measurement

DOI: 10.1021/cn900016z | *ACS Chem. Neurosci.* (2010), *1*, 182–193

of [Ca2+]o fluctuations with calcium-selective microelectrodes. *Eur. J. Neurosci. 3*, 10–17.

47. Keicher, E., Maggio, K., Hernandez-Nicaise, M. L., and Nicaise, G. (1991) The lacunar glial zone at the periphery of *Aplysia* giant neuron: Volume of extracellular space and total calcium content of gliagrana. *Neuroscience 42*, 593–601.

48. Keicher, E., Maggio, K., Hernandez-Nicaise, M. L., and Nicaise, G. (1992) The abundance of *Aplysia* gliagrana depends on Ca2+ and/or Na+ concentrations in sea water. *Glia 5*, 131–138.

49. Coggeshall, R. E. (1967) A light and electron microscope study of the abdominal ganglion of *Aplysia californica*. *J. Neurophysiol. 30*, 1263–1287.

50. Rosenbluth, J. (1963) The visceral ganglion of *Aplysia californica*. *Z. Zellforsch. Mikrosk. Anat. 60*, 213–236.

51. Burette, A., Zabel, U., Weinberg, R. J., Schmidt, H. H., and Valtschanoff, J. G. (2002) Synaptic localization of nitric oxide synthase and soluble guanylyl cyclase in the hippocampus. *J. Neurosci. 22*, 8961–8970.

52. Roychowdhury, S., Luthe, A., Keilhoff, G., Wolf, G., and Horn, T. F. (2002) Oxidative stress in glial cultures: Detection by DAF-2 fluorescence used as a tool to measure peroxynitrite rather than nitric oxide. *Glia 38*, 103–114.

53. Bicker, G. (2005) STOP and GO with NO: Nitric oxide as a regulator of cell motility in simple brains. *Bioessays 27*, 495–505.

54. Moroz, L. L., Norby, S. W., Cruz, L., Sweedler, J. V., Gillette, R., and Clarkson, R. B. (1998) Non-enzymatic production of nitric oxide (NO) from NO synthase inhibitors. *Biochem. Biophys. Res. Commun. 253*, 571–576.

55. Boudko, D. Y., Cooper, B. Y., Harvey, W. R., and Moroz, L. L. (2002) High-resolution microanalysis of nitrite and nitrate in neuronal tissues by capillary electrophoresis with conductivity detection. *J. Chromatogr. B: Anal. Technol. Biomed. Life Sci. 774*, 97–104.

56. Cruz, L., Moroz, L. L., Gillette, R., and Sweedler, J. V. (1997) Nitrite and nitrate levels in individual molluscan neurons: Single-cell capillary electrophoresis analysis. *J. Neurochem. 69*, 110–115.

57. Moroz, L. L., Dahlgren, R. L., Boudko, D., Sweedler, J. V., and Lovell, P. (2005) Direct single cell determination of nitric oxide synthase related metabolites in identified nitrergic neurons. *J. Inorg. Biochem. 99*, 929–939.

58. Flaster, M. S., Ambron, R. T., and Schacher, S. (1986) Growth cones isolated from identified *Aplysia* neurons *in vitro*: Biochemical and morphological characterization. *Dev. Biol. 118*, 577–586.

59. Moroz, L. L., Ju, J., Russo, J. J., Puthanveetti, S., Kohn, A., Medina, M., Walsh, P. J., Birren, B., Lander, E. S., Kandel, E. R. (2006) Proposal to Sequence the Genome of Aplysia californica. See http://www.genome.gov/Pages/Research/Sequencing/SeqProposals/AplysiaSeq.pdf.

60. Floyd, P. D., Moroz, L. L., Gillette, R., and Sweedler, J. V. (1998) Capillary electrophoresis analysis of nitric oxide synthase related metabolites in single identified neurons. *Anal. Chem. 70*, 2243–2247.

61. Kim, W. S., Dahlgren, R. L., Moroz, L. L., and Sweedler, J. V. (2002) Ascorbic acid assays of individual neurons and neuronal tissues using capillary electrophoresis with laser-induced fluorescence detection. *Anal. Chem. 74*, 5614–5620.

DOI: 10.1021/cn900016z | *ACS Chem. Neurosci.* (2010), *1*, 182–193